The EMBO Journal (2007) 26, 3144–3156 | © 2007 European Molecular Biology Organization | All Rights Reserved 0261-4189/07
www.embojournal.org

THE EMBO JOURNAL

Drosophila Omi, a mitochondrial-localized IAP antagonist and proapoptotic serine protease

Madhavi Challa[1,2,5], Srinivas Malladi[1,2,5], Brett J Pellock[3], Douglas Dresnek[3], Shankar Varadarajan[1,2], Y Whitney Yin[2,4], Kristin White[3] and Shawn B Bratton[1,2,*]

[1]Division of Pharmacology and Toxicology, College of Pharmacy, The University of Texas at Austin, Austin, TX, USA, [2]Institute for Cellular and Molecular Biology, The University of Texas at Austin, Austin, TX, USA, [3]Cutaneous Biology Research Center, Massachusetts General Hospital, Harvard Medical School, Charlestown, MA, USA and [4]Department of Chemistry and Biochemistry, The University of Texas at Austin, Austin, TX, USA

Although essential in mammals, in flies the importance of mitochondrial outer membrane permeabilization for apoptosis remains highly controversial. Herein, we demonstrate that *Drosophila* Omi (dOmi), a fly homologue of the serine protease Omi/HtrA2, is a developmentally regulated mitochondrial intermembrane space protein that undergoes processive cleavage, *in situ*, to generate two distinct inhibitor of apoptosis (IAP) binding motifs. Depending upon the proapoptotic stimulus, mature dOmi is then differentially released into the cytosol, where it binds selectively to the baculovirus IAP repeat 2 (BIR2) domain in *Drosophila* IAP1 (DIAP1) and displaces the initiator caspase DRONC. This interaction alone, however, is insufficient to promote apoptosis, as dOmi fails to displace the effector caspase DrICE from the BIR1 domain in DIAP1. Rather, dOmi alleviates DIAP1 inhibition of all caspases by proteolytically degrading DIAP1 and induces apoptosis both in cultured cells and in the developing fly eye. In summary, we demonstrate for the first time in flies that mitochondrial permeabilization not only occurs during apoptosis but also results in the release of a bona fide proapoptotic protein.

The EMBO Journal (2007) **26,** 3144–3156. doi:10.1038/sj.emboj.7601745; Published online 7 June 2007
Subject Categories: differentiation & death
Keywords: apoptosis; DIAP1; dOmi; DRONC; *Drosophila*

Introduction

Apoptosis, or programmed cell death, is an evolutionarily conserved process that is required for normal development and homeostasis of most (if not all) metazoans (Danial and Korsmeyer, 2004; Kornbluth and White, 2005). Cysteinyl aspartate-specific proteases (caspases) are generally activated during apoptosis and are responsible for the biochemical and morphological features commonly associated with this form of cell death. Consequently, the mechanisms that mediate the activation of caspases and/or regulate their activities are of considerable interest (Fuentes-Prior and Salvesen, 2004). In mammals, cellular stress often results in mitochondrial outer membrane permeabilization (MOMP), which facilitates the release of cytochrome *c* from the intermembrane space into the cytosol. Cytochrome *c* then binds to the adapter protein, apoptotic protease-activating factor-1 (Apaf-1), and in the presence of dATP or ATP, stimulates oligomerization of Apaf-1 into a large ~700–1400 kDa apoptosome complex that sequentially recruits and activates the initiator caspase-9 and the effector caspase-3 (Cain *et al*, 2002).

Given the importance of MOMP for apoptosis, both proapoptotic (e.g., Bim, Bid, Bax, and Bak) and antiapoptotic (e.g., Bcl-2, Bcl-x_L, and Mcl-1) Bcl-2 family members have evolved to tightly regulate this process (Danial and Korsmeyer, 2004). Nevertheless, in the event that caspases are activated, a second layer of protection also exists, comprised of the inhibitor of apoptosis (IAP) proteins (Salvesen and Duckett, 2002). Originally identified in baculoviruses, where they serve to inhibit host cell death during viral replication, IAPs are characterized by the presence of one or more baculovirus IAP repeat (BIR) domains and in some cases, a C-terminal RING domain that functions as an E3 ubiquitin ligase. X-linked IAP (XIAP), the prototypical IAP in mammals, binds to and potently inhibits the activities of caspases-9 and -3 via its BIR3 and linker-BIR2 domains, respectively, and may in turn catalyze the ubiquitinylation and turnover of caspases via the 26S proteasome (Salvesen and Duckett, 2002).

By contrast, in flies, previous studies suggest that MOMP does not occur, and that cytochrome *c* is not released into the cytosol in response to stress (Varkey *et al*, 1999; Zimmermann *et al*, 2002; Dorstyn *et al*, 2004), despite the existence of both proapoptotic (Debcl/dBorg-1/Drob-1/dBok) and antiapoptotic (Buffy/dBorg-2) Bcl-2 family members (Igaki and Miura, 2004). Moreover, the Apaf-1 homologue, *Drosophila* Apaf-1-related killer (DARK/Hac-1/dApaf), reportedly does not require cytochrome *c* for its activation and is constitutively active in cells, where it binds to and continuously processes the initiator caspase DRONC (Muro *et al*, 2002; Zimmermann *et al*, 2002; Dorstyn *et al*, 2004). Other reports, however, suggest that cytochrome *c* can bind to DARK, and that it is required for DARK-dependent activation of caspases, at least during spermatid individualization and developmental apoptosis in the fly eye (Kanuka *et al*, 1999; Arama *et al*, 2003, 2006; Mendes *et al*, 2006). Thus, in flies, the specific roles that mitochondrial proteins play in apoptosis remain highly controversial (Means *et al*, 2006). Regardless, once formed, the DARK·DRONC apoptosome complex is held in check by *Drosophila* IAP1 (DIAP1), which binds via its BIR2 domain to the linker region separating the prodomain

*Corresponding author. Division of Pharmacology and Toxicology, College of Pharmacy, The University of Texas at Austin, 1 University Station A1915, 2409 University Avenue, Austin, TX 78712-0125, USA. Tel.: +1 512 471 1735; Fax: +1 512 471 5002;
E-mail: sbbratton@mail.utexas.edu
[5]These authors contributed equally to this work

Received: 31 January 2007; accepted: 10 May 2007; published online: 7 June 2007

and the large subunit (protease domain) of DRONC (Meier *et al*, 2000; Chai *et al*, 2003). Intriguingly, DIAP1 apparently does not directly inhibit DRONC activity, but instead promotes its turnover in the cell through ubiquitinylation (Wilson *et al*, 2002; Chai *et al*, 2003).

Consistent with its central role in regulating apoptosis, mutations in DIAP1 that diminish its interaction with caspases, consequently enhance or induce apoptosis (Hay *et al*, 1995; Goyal *et al*, 2000; Lisi *et al*, 2000). Moreover, a number of *Drosophila* IAP (DIAP) antagonists have been discovered, including Reaper (Rpr), head involution defective (Hid), Grim, and Sickle, that are either transcriptionally upregulated or post-translationally modified in response to specific developmental cues or stressful stimuli (Kornbluth and White, 2005). Each of these IAP antagonists possesses an N-terminal IAP binding motif (IBM) that displaces active caspases from DIAP1 and/or induces DIAP1 autoubiquitinylation, resulting in the induction of apoptosis (Kornbluth and White, 2005). In sharp contrast, the mammalian IAP antagonists, Smac/DIABLO and Omi/HtrA2, are constitutively expressed and sequestered to the mitochondrial intermembrane space before stress-induced MOMP (Du *et al*, 2000; Verhagen *et al*, 2000, 2001; Hegde *et al*, 2001; Martins *et al*, 2001; Suzuki *et al*, 2001). Thus, it could be reasonably argued that MOMP may not be required for apoptosis in flies, because their IAP antagonists are not sequestered to mitochondria.

Recent studies however indicate that Rpr and Grim contain a second conserved motif, referred to as the Trp-block or GH3 domain, which mediates their relocalization to mitochondria and is required for efficient cell killing (Wing *et al*, 2001; Claveria *et al*, 2002; Olson *et al*, 2003). Moreover, there is precedence for the sequestration of IAP antagonists in the fly, as Jafrac2 is initially localized to the endoplasmic reticulum (ER), before its release during ER stress (Tenev *et al*, 2002). Thus, we sought to further investigate the putative role(s) of mitochondrial proteins in fly apoptosis and report here the identification and characterization of *Drosophila* Omi (dOmi), the first mitochondrial-sequestered dual IAP antagonist and proapoptotic serine protease in flies.

Results

dOmi is a Drosophila Omi/HtrA2 homologue

A TBLASTN search of the *Drosophila* sequence database (FlyBase) was performed using human Omi/HtrA2 (hOmi; amino acids 1–458). This resulted in identification of a putative *omi*-like homologue (gene CG8464), which mapped to region 88C3 on chromosome arm 3R and contained three exons spanning ~1.8 kb, including a 286-bp 5′-UTR, a 1270-bp coding region, and a 92-bp 3′-UTR (Figure 1A). A full-length EST (AT14262) was subsequently obtained, and the entire open reading frame cloned into both insect and bacterial expression plasmids. Expression of *domi* confirmed that it encoded a 422 amino-acid protein with a molecular mass of ~46 kDa (see below). Alignment of dOmi with several members of the HtrA family revealed significant homology, particularly within the serine protease and PDZ domains, where dOmi shares ~57 and ~45% identity with hOmi, respectively (Figure 1B). Moreover, threading of the dOmi sequence onto the structure of hOmi suggested significant overall structural similarity (Figure 1C; PDB code 1LCY) (Li *et al*, 2002).

dOmi contains an N-terminal targeting sequence that is proteolytically removed during mitochondrial import

hOmi, a class I intermembrane space protein, contains a mitochondrial targeting sequence (MTS) that mediates its import across the outer mitochondrial membrane, as well as its insertion into the inner mitochondrial membrane (Figure 2A). Analysis of the dOmi sequence using the PSORTII program suggested that dOmi also possessed a putative N-terminal MTS. Therefore, we transiently transfected *Drosophila* S2 cells with a C-terminal, myc-tagged version of dOmi and examined the cells by immunofluorescence microscopy. As predicted, both dOmi-myc and cytochrome *c* (positive control) were found exclusively in mitochondria, as indicated by their colocalization with Mitotracker® Red (Figure 2B). Immunoblotting of the dOmi-myc transfected cells subsequently revealed that, following its import into mitochondria, dOmi underwent N-terminal processing at two sites, resulting in the generation of two distinct dOmi fragments (~37 and ~35 kDa) (Figure 2C, lane 2). A hydrophobicity plot of dOmi's N-terminus indicated the presence of a putative transmembrane domain (amino acids 63–82)—likely utilized for insertion into the inner mitochondrial membrane (Figure 2A)—as well as a second hydrophobic patch (amino acids 100–120) that was highly homologous to the trimerization domain previously described for hOmi (Figures 1B and 2D) (Li *et al*, 2002). We therefore speculated that cleavage of dOmi might occur within the region separating these two hydrophobic motifs. Further analysis using the SignalP program predicted cleavage at $A^{79}\downarrow$AIIQ, and we noted a second di-alanine motif at $A^{92}\downarrow$ASKM (Figure 2D). Since cleavage at these two sites would yield dOmi fragments of ~37 and ~35 kDa, respectively, we mutated each pair of alanines to aspartic acids in an effort to inhibit proteolytic processing.

As anticipated, mutation of Ala92 and Ala93 to aspartic acids almost entirely prevented formation of the 35 kDa dOmi fragment (Figure 2C, lane 4). Similarly, mutation of Ala79 and Ala80 to aspartic acids prevented formation of the 37 kDa dOmi fragment; however, the negatively charged aspartic acid residues disrupted the adjacent transmembrane domain and brought about unnatural processing of dOmi at another site (data not shown). We therefore generated an A79W/A80W mutant, which preserved the overall hydrophobicity of the putative cleavage site but, due to the increased size of the tryptophan residues, completely prevented processing and formation of the 37 kDa dOmi fragment (Figure 2C, lane 3). Interestingly, the A79W/A80W mutant also exhibited reduced processing at the $A^{92}\downarrow$ASKM site, which suggested that dOmi was initially processed to the 37 kDa fragment, followed by secondary processing to the 35 kDa fragment. dOmi did not appear to undergo autocatalytic cleavage at either site, since the active-site serine mutant S266A failed to inhibit processing of the enzyme (data not shown). In any event, mutation of all four alanine residues (A79W/A80W/A92D/A93D) resulted in essentially a noncleavable mutant of dOmi (Figure 2C, lane 5). The minor cleavage products that were observed likely resulted from promiscuous cleavage of dOmi by its signal peptide protease complex. Since proteolytic processing of mitochondrial proteins often results in the removal of their MTS residues, we next expressed the Δ79 and Δ92 mature forms of dOmi-myc in S2 cells (corresponding to the

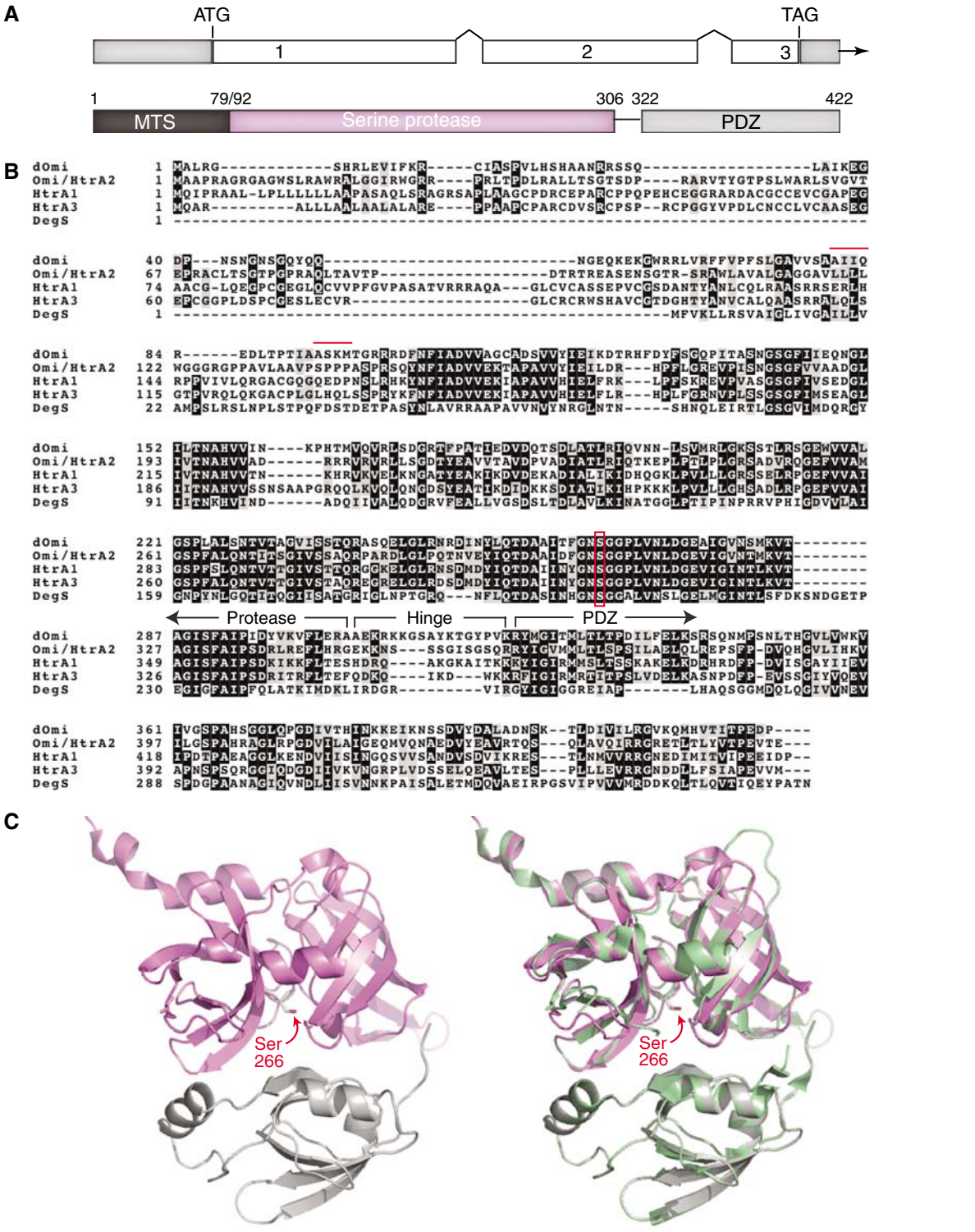

Figure 1 dOmi is an HtrA family member. (**A**) *domi* contains three exons spanning ~1.8 kb, including a 286-bp 5′-UTR (gray), a 1270-bp coding region, and a 92-bp 3′-UTR (gray). The protein sequence contains an N-terminal MTS, a serine protease domain, a hinge region, and a PDZ protein interaction domain. (**B**) The coding sequence of dOmi was aligned (ClustalW) with human HtrA1, Omi/HtrA2, HtrA3, and bacterial DegS. Red bars indicate dOmi's two IBMs; the red box indicates the conserved active-site serines present in all HtrA family members. (**C**) A structural model of dOmi was created by threading its primary amino-acid sequence onto the solved crystal structure of human Omi. dOmi, with its serine protease (pink) and PDZ (gray) domains, is shown either alone (left structure) or threaded with human Omi (green, right structures).

37 and 35 kDa fragments, respectively) and analyzed them by fluorescence microscopy. As anticipated, removal of these N-terminal residues from dOmi prevented its import into mitochondria, as dOmi no longer colocalized with Mitotracker® Red and instead remained present within the cytoplasm (Figure 2B).

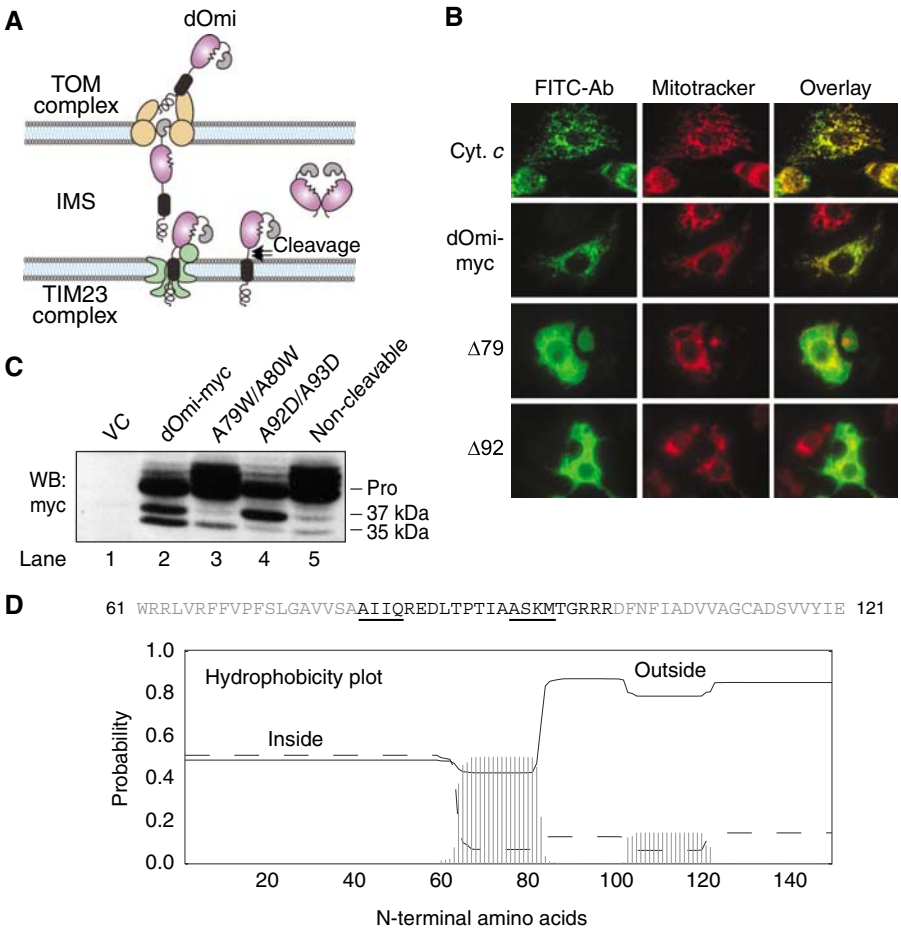

Figure 2 dOmi is a mitochondrial protein that is imported and processed at two sites within the intermembrane space. (**A**) Model of dOmi import across the outer mitochondrial membrane and processing within the intermembrane space (IMS). TOM/TIM23 complexes are located on the outer and inner mitochondrial membranes, respectively. (**B**) S2 cells were transiently transfected with either full-length, Δ79 or Δ92-dOmi-myc for 24 h and stained with primary anti-myc or anti-cytochrome *c* (positive control) antibodies, followed by a secondary FITC-labeled anti-mouse antibody. Mitochondrial localization was determined by staining cells with Mitotracker® Red. (**C**) S2 cells were transfected with full-length wild-type dOmi-myc, or various cleavage site mutants, for 24 h and then immunoblotted using an anti-myc antibody. (**D**) A hydrophobicity plot of the N-terminus (residues 1–150) of dOmi was generated using the TMHMM Server v. 2.0 (CBS; Denmark). The inside/outside probability determinations indicate that residues 82–140 are located on the same side of the intermembrane, facing the IMS.

Mature dOmi contains two IBMs and is developmentally regulated in flies

Proteolytic removal of the MTS from hOmi not only liberates the enzyme from its inner mitochondrial membrane anchor (Figure 2A), but also exposes a cryptic IBM that is required for its interaction with XIAP (Hegde *et al*, 2001; Martins *et al*, 2001; Suzuki *et al*, 2001; Verhagen *et al*, 2001). Anecdotal reports have suggested that homologues of hOmi do not contain IBMs, primarily because the AVPS motif in hOmi is not conserved in other species, including *Drosophila* (Figure 1B). However, the fact that dOmi underwent cleavage at two distinct di-alanine motifs raised the possibility that it might contain functional IBMs. Indeed, Δ79-dOmi contained an N-terminal AIIQ motif that was similar to that observed for the known IAP antagonists Grim and Sickle, and Δ92-dOmi contained an ASKM motif with the requisite N-terminal alanine, as well as a preferred hydrophobic residue in the P_4 position (Figure 3A). We therefore performed *in vitro* pull-down assays using highly purified GST-DIAP1, and either recombinant Δ79-dOmi or Δ92-dOmi. As shown in Figure 3B, DIAP1 bound each of the cleaved forms of dOmi (lanes 3, 5, 9, and 11), but failed to do so when the corresponding IBMs (AIIQ and ASKM) were removed (lanes 4 and 6), or when the first two amino acids were mutated to glycines (lanes 10 and 12). Thus, proteolytic removal of the MTS from dOmi resulted in the formation of two fragments, both of which possessed N-terminal IBMs capable of binding to DIAP1.

To verify that processing of endogenous dOmi occurred within mitochondria and resulted in the generation of IAP antagonists in flies, we prepared lysates from wild-type embryos (12 h) and performed DIAP1 pull-down assays using various subcellular fractions. DIAP1 precipitates were then immunoblotted with a rabbit polyclonal antibody raised against recombinant Δ79-dOmi. As expected, DIAP1-bound dOmi fragments were isolated exclusively from the mitochondrial fraction (Figure 3C). We then prepared lysates from embryos (12 h), larvae (second instar), pupae, and adult flies, as well as S2 cells, and once again performed pull-down assays using GST-DIAP1 (Supplementary methods). Intriguingly, we found that the expression of dOmi fluctuated, depending upon the developmental stage of the flies. dOmi expression levels were initially high in embryos, but declined

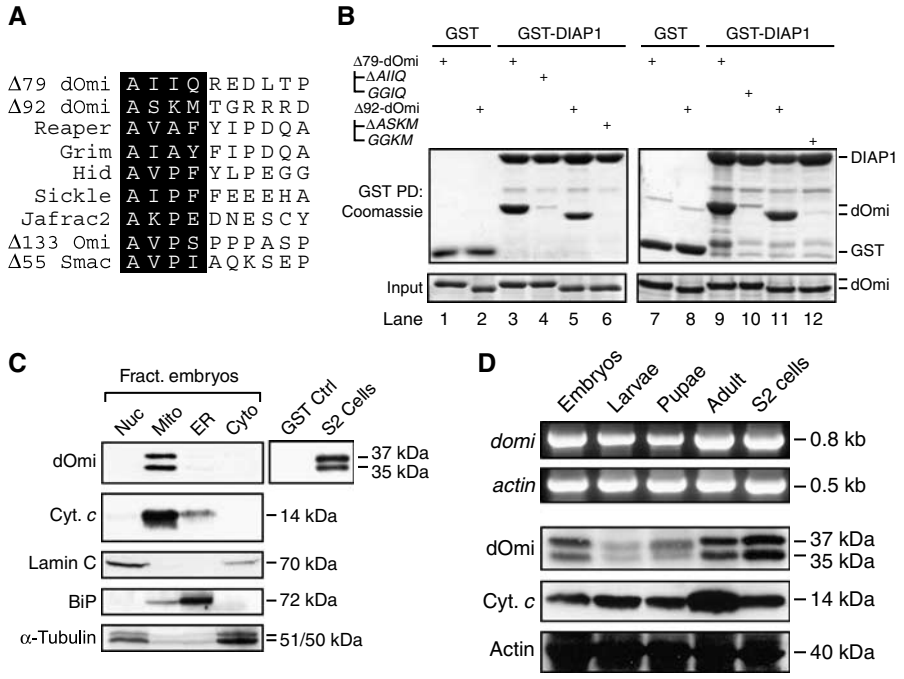

Figure 3 Mature dOmi binds DIAP1 via two distinct IBMs and is developmentally regulated *in vivo*. (**A**) The IBMs in Δ79-dOmi and Δ92-dOmi were aligned with known IAP antagonists in *Drosophila* (Reaper, Grim, Hid, Sickle, Jafrac2) and humans (Δ133-hOmi, Δ55-Smac). (**B**) GST-DIAP1 pull-down assays were performed using recombinant Δ79-dOmi and Δ92-dOmi, as well as their corresponding IBM truncations (Δ*AIIQ,* Δ*ASKM*) or point mutants (*GGIQ, GGKM*), respectively. Each of the dOmi proteins also contained an active-site mutation (S266A). Isolated protein complexes were separated by SDS–PAGE, and the gels stained with Coomassie Blue. (**C**) Subcellular fractions were isolated from fly embryo (12 h) lysates and incubated with GST-DIAP1. DIAP1 complexes from each fraction were then washed and immunoblotted for endogenous dOmi, using a rabbit polyclonal antibody raised against recombinant dOmi. Each fraction was also immunoblotted for cytochrome *c*, lamin C, BiP, and α-tubulin, in order to verify the purity of the fraction. (**D**) Lysates from embryos (12 h), larvae (second instar), pupae, and adult flies were immunoblotted for cytochrome *c* and endogenous dOmi (as described in panel C). Total RNA was also isolated at each developmental stage and subjected to RT–PCR for *domi* and *actin* (internal control).

during the larval and pupal stages, only to rebound in the adult flies (Figure 3D). The observed changes in dOmi expression could not be accounted for by differences in total mitochondrial density, as cytochrome *c* levels were increased only in the adult flies (Figure 3D). We performed RT–PCR on total RNA isolated from each tissue sample and correspondingly observed that *domi* expression was slightly reduced in both larvae and pupae (Figure 3D). It is currently unclear why dOmi expression levels change during development, or if additional posttranslational modifications (e.g. ubiquitinylation) may also enhance its turnover.

Mature dOmi is released from mitochondria during apoptosis via caspase-dependent and -independent mechanisms

As previously noted, the role of mitochondria in fly apoptosis remains highly controversial, in part because some previous reports suggest that mitochondria do not undergo outer membrane permeabilization and that cytochrome *c* is not required for activation of the DARK·DRONC apoptosome complex (Varkey *et al*, 1999; Zimmermann *et al*, 2002; Dorstyn *et al*, 2004). Therefore, in order to determine if cytochrome *c* was released from mitochondria during apoptosis, we treated S2 cells with the general serine/threonine kinase inhibitor staurosporine (STS) or exposed them to DNA damaging UVB irradiation. In each case, we observed the release of cytochrome *c* from mitochondria, a loss in mitochondrial membrane potential ($\Delta\psi_m$), an increase in effector caspase DEVDase activity, and DNA fragmentation (Sub-G1 peak) (Figure 4A and B). Similarly, in cells transfected with full-length dOmi-myc, STS and UVB irradiation also stimulated the release of both Δ79-dOmi and Δ92-dOmi, along with cytochrome *c* (Figure 4C), and once in the cytosol, mature dOmi enhanced effector caspase DEVDase activity (Figure 4D). Correspondingly, in loss-of-function experiments, depletion of dOmi by RNA interference delayed caspase activation (Figure 4E).

Interestingly, pretreatment of cells with the pancaspase inhibitor benzyloxycarbonyl-Val-Ala-Asp-(OMe)fluoromethyl ketone (Z-VAD-fmk) inhibited all of the aforementioned events in UVB-irradiated cells, including the release of cytochrome *c* and dOmi, but failed to do so in STS-treated cells (Figure 4A–C). Thus, depending upon the proapoptotic stimulus, both cytochrome *c* and dOmi were released from mitochondria via caspase-dependent and -independent mechanisms, the precise details of which remain to be elucidated. Notably, UVB irradiation selectively induces expression of DARK in early-stage embryos (Zhou and Steller, 2003). Therefore, it is possible that DRONC, or perhaps its downstream targets, DrICE or DCP-1, may be required for MOMP in this context.

Mature dOmi induces cell death in S2 cells and in the developing fly eye, primarily through its serine protease activity

Although dOmi was released from mitochondria during apoptosis, it remained unclear precisely how cytoplasmic dOmi might induce apoptosis in *Drosophila* cells. We there-

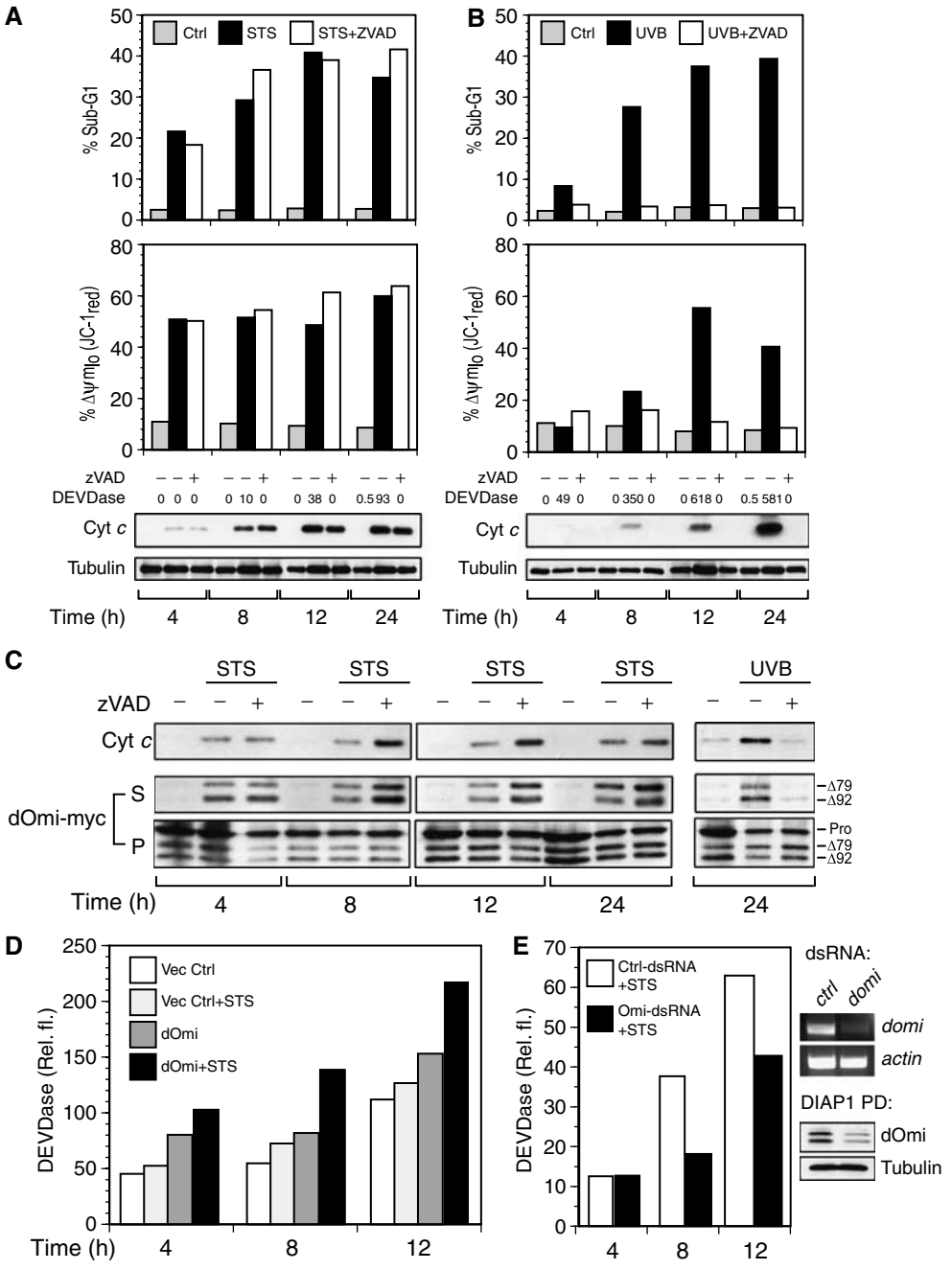

Figure 4 STS and UVB irradiation induce caspase-dependent and -independent MOMP in S2 cells. S2 cells were exposed to STS (1 μM) or UVB irradiation (5 min on a UV transilluminator), in the presence or absence of the pancaspase inhibitor Z-VAD-fmk (50 μM). (**A**, **B**) Cells were subsequently examined for Δψm (JC-1 staining) and DNA fragmentation (Sub-G1 peak). In addition, cytosolic fractions were prepared and immunoblotted for cytochrome *c* and assayed for effector caspase DEVDase activity. (**C**, **D**) Similarly, cells were transfected with full-length dOmi, exposed to STS or UVB irradiation, and examined for mitochondrial release of cytochrome *c* and dOmi into the cytosol, as well as effector caspase DEVDase activity. (**E**) S2 cells (0.3×10^6) were pretreated with control or *domi* dsRNA (40 nM) for 3 days, exposed to STS (1 μM) for 4–12 h, and subsequently assayed for effector caspase DEVDase activity. To confirm the extent of knockdown by RNA interference, dOmi mRNA and protein expression levels were determined by RT–PCR and Western blotting (inset).

fore expressed mature Δ79-dOmi or Δ92-dOmi in the cytoplasm of S2 cells (Figure 2B), and found that both forms induced ~40% cell death by 48 h (Figure 5A, WT versus Vec Ctrl). Interestingly, however, the IBM mutants Δ79-dOmi^{GGIQ} and Δ92-dOmi^{GGKM} triggered similar levels of cell death compared to wild-type dOmi (Figure 5A, WT versus IBM Mt), despite their inability to bind DIAP1 (Figure 3B). Moreover, mutation of dOmi's catalytic serine reduced cell death (Figure 5A, WT versus S266A), whereas removal of its regulatory PDZ domain (which provides greater access to its active site) significantly enhanced cell death (Figures 1C and 5A, WT versus ΔPDZ). Thus, dOmi's serine protease activity appeared to be primarily responsible for inducing cell death in S2 cells. Pretreatment of cells with Z-VAD-fmk partially inhibited cell death induced by the catalytically active forms (WT, ΔPDZ, IBM Mt) of dOmi (Figure 5A), indicating that

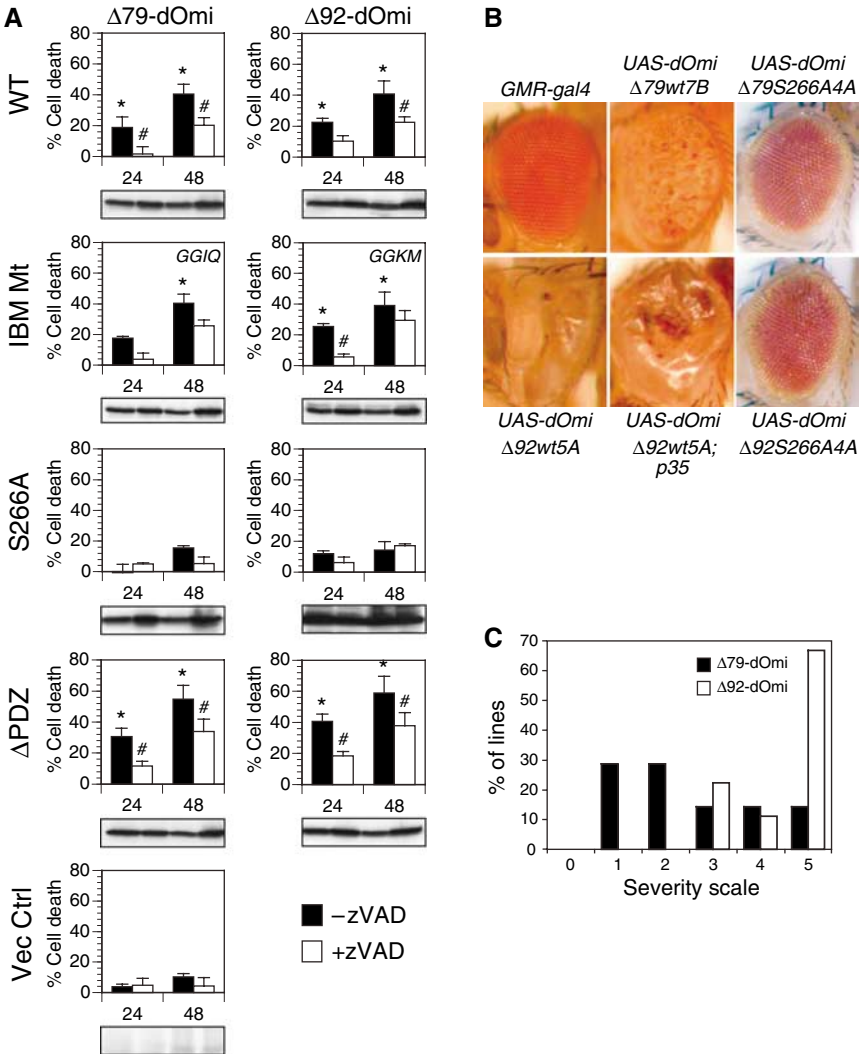

Figure 5 Mature dOmi induces cell death in S2 cells and the developing fly eye. (**A**) S2 cells were cotransfected with expression plasmids for EGFP and wild-type dOmi (Δ*79-dOmi*, Δ*92-dOmi*), or various IBM mutants (Δ*79-dOmi*^{GGIQ}, Δ*92-dOmi*^{GGKM}), catalytically inactive mutants (Δ*79-dOmi*^{S266A}, Δ*92-dOmi*^{S266A}), or PDZ truncation mutants (Δ*79-dOmi*Δ^{PDZ}, Δ*92-dOmi*Δ^{PDZ}). All dOmi constructs were expressed under the control of the metallothionein promoter by adding $CuSO_4$ (0.7 mM) to the culture medium, in the presence and absence of Z-VAD-fmk (50 μM). Cell death was assessed by determining the percent of GFP$^+$ cells remaining at 24 and 48 h. For statistical analyses, ANOVA was performed, along with a Student–Newman–Keuls *post hoc* analysis (StatView software): *significantly different from the Vec Ctrl ($P<0.05$); #, significantly different from cells not treated with Z-VAD-fmk ($P<0.05$). (**B**) Expression of Δ79-dOmi resulted in phenotypes ranging from early pupal lethality in some lines to a mild, slightly rough eye in other lines (as shown: *GMR-gal4/+; UAS-Δ79-dOmi7B*). Expression of Δ92-dOmi resulted in consistently stronger phenotypes, ranging from early pupal lethality in some lines to eyeless flies in other lines (as shown: *GMR-gal4/+; Δ92-dOmi5A/+*). Coexpression of the baculoviral caspase inhibitor p35 failed to significantly inhibit cell death induced by Δ79-dOmi or Δ92-dOmi (as shown: *GMR-gal4/UAS-p35; Δ92-dOmi5A/+*), and expression of the catalytically inactive dOmi mutants failed to induce cell death (as shown: *GMR-gal4/+; UAS-Δ79-dOmiS266A4A and GMR-gal4/+; UAS-Δ92-dOmiS266A42A*). (**C**) Transgenic lines were crossed to GMR-gal4 and scored for phenotype, based on the following scale: 0, no phenotype; 1, some viable, late pigment cell death; 2, some viable, moderate reduction in eye size; 3, some viable, no eye or very small eye; 4, lethal at pharate adult stage; 5, lethal at early pupal stage. Nine independent lines were scored for Δ92-dOmi and seven for Δ79-dOmi, and each line was tested at least twice and produced at least 10 flies with the same phenotype. Expression of Δ92-dOmi consistently resulted in a more severe phenotype ($P<0.02$, Student's *t*-test).

dOmi's proteolytic activity could promote the activation of caspases and induce caspase-dependent apoptosis. However, dOmi, like its mammalian counterpart, also induced caspase-independent cell death (Hegde *et al*, 2001).

To determine if dOmi could induce cell death in the developing fly eye, we generated transgenic flies expressing wild-type Δ79-dOmi (*GMR-gal4*;*UAS-domi*Δ*79wt7B*), Δ92-dOmi (*GMR-gal4*;*UAS-domi*Δ*92wt5A*), or their catalytically inactive S266A mutants (*GMR-gal4*;*UAS-dOmi*Δ*79S266A4A* and *GMR-gal4*;*UAS-dOmi*Δ*92S266A42A*). Interestingly, when compared with control flies, expression of Δ79-dOmi and Δ92-dOmi resulted in phenotypes ranging from organismal lethality at pupal stages to a rough eye (Figure 5B and C). The effects of Δ92-dOmi were consistently much stronger than Δ79-dOmi (Figure 5C), but as previously observed in S2 cells, expression of the catalytically inactive S266A dOmi mutants did not result in any phenotype (Figure 5B). In contrast to the effects of Z-VAD-fmk in S2 cells, expression of the baculoviral caspase inhibitor p35 did not inhibit cell death induced by Δ79-dOmi or Δ92-dOmi (Figure 5B, data not shown).

GMR-driven expression of dOmi in the fly eye however occurred over a ~5–6 day period, beginning with photoreceptor differentiation in the third larval instar and continuing throughout pupal development, whereas the effects of dOmi expression in S2 cells were examined after 1–2 days. Thus, dOmi could promote caspase-dependent apoptosis via its serine protease activity, but in the long term did not require caspase activity in order to induce cell death.

The IBMs in dOmi interact selectively with the BIR2 domain in DIAP1 and displace the initiator caspase DRONC

Rpr, Hid, Grim, Sickle, and Jafrac2 all reportedly induce apoptosis in the fly, by interacting with and displacing the effector caspase DrICE from the BIR1 domain in DIAP1, and/or the initiator caspase DRONC from the BIR2 domain (Chai *et al*, 2003; Zachariou *et al*, 2003; Yan *et al*, 2004). Therefore, since dOmi clearly bound to DIAP1 in an IBM-dependent manner (Figure 3B), it was surprising that this interaction alone failed to induce significant amounts of apoptosis in S2 cells or in the developing fly eye (Figure 5A, S266A versus Vec Ctrl, Figure 5B). In order to resolve this dilemma, we sought to further characterize dOmi's interaction with DIAP1, as well as its role in promoting caspase activation. We began by expressing various DIAP1 truncation mutants as GST fusion proteins and subsequently performed pulldown assays using naïve S2 cell lysates (Figure 6A and B). Importantly, the BIR2 domain in DIAP1 was found to be essential for binding both processed forms of endogenous dOmi, whereas neither the BIR1 nor the RING domains were required (Figure 6B).

Given that dOmi failed to bind BIR1, we predicted that it would be unable to antagonize BIR1-dependent inhibition of DrICE. To provide definitive evidence, we incubated recombinant DrICE with its substrate PARP, either alone or in the presence of GST-BIR1. At its approximate IC_{50}, GST-BIR1 inhibited DrICE-mediated cleavage of PARP by ~50% (Figure 6C and D, lanes 1–3). As expected, this inhibition was readily overcome by a Rpr peptide, matching its N-terminal IBM (Rpr-IBM; AVAFYIPD), but not by a control peptide (MKSDFYFQ) (Figure 6D, lanes 4 and 6). More importantly, however, neither recombinant Δ79-dOmi, Δ92-dOmi, nor their IBM truncation mutants (ΔAIIQ or ΔASKM), promoted DrICE-dependent cleavage of PARP (Figure 6C, lanes 4–7). Moreover, unlike Rpr-IBM, the IBM peptide of Δ79-dOmi (AIIQREDL) also failed to antagonize BIR1-dependent inhibition of DrICE (Figure 6D, lanes 4 and 5). To determine why dOmi failed to displace DrICE, we modeled the Δ79-IBM into the BIR1 binding pocket of DIAP1, using the previously solved crystal structure for BIR1 bound to Rpr-IBM (PDB code 1SDZ; Yan *et al*, 2004). As shown in Figure 6E, Arg5 in dOmi appeared to sterically clash with Glu86 in the bottom of the BIR1 pocket, thus preventing Δ79-dOmi from forming a stable complex with BIR1.

Since mature dOmi bound to the BIR2 domain in DIAP1 (Figure 6B), we predicted that dOmi might displace the initiator caspase DRONC from the BIR2 binding pocket. We therefore incubated GST-BIR2-RING with an N-terminal fragment of DRONC (1–139) and observed the formation of a BIR2-RING·DRONC complex (Figure 7A, lanes 1 and 10), consistent with a previous report (Chai *et al*, 2003). As expected, addition of Δ79-dOmi or Δ92-dOmi to the incubation mixture resulted in a concentration-dependent displacement of DRONC from the complex (Figure 7A, lanes 2–5 and 11–14), with Δ79-dOmi displaying a higher affinity for BIR2-RING compared to Δ92-dOmi (K_d ~0.27 μM versus ~1.18 μM) (Figure 7C). By contrast, neither of the IBM truncation mutants (ΔAIIQ or ΔASKM) bound to BIR2-RING or displaced DRONC (Figure 7A, lanes 6–9 and 15–18). In additional experiments, the Rpr-IBM peptide also displaced DRONC from the BIR2 binding pocket (Figure 7B), with an affinity similar to that reported for the Hid-IBM (K_d ~0.036 μM versus 0.041 μM) (Figure 7C) (Wu *et al*, 2001). Thus, in our assays, Rpr was ~7-fold more potent than Δ79-dOmi at displacing DRONC (Figure 7C). Nevertheless, the affinity of Δ79-dOmi for DIAP1-BIR2 was ~3-fold higher than that reported for DRONC (Figure 7C) (Chai *et al*, 2003). Moreover, by comparison, the affinity of Δ79-dOmi for DIAP1-BIR2 was higher than that reported for Smac with XIAP-BIR3 (Liu *et al*, 2000), which is compelling, given that DRONC and caspase-9 exhibit virtually identical binding affinities for their respective IAPs (Figure 7C).

The reasons for the selectivity of Δ79-dOmi for BIR2 over BIR1 were subsequently revealed through modeling studies, using the solved crystal structure of BIR2 bound to Hid-IBM (PDB code 1JD6) (Wu *et al*, 2001) (Figure 7D). Indeed, the steric clash observed between Arg5 in Δ79-dOmi and Glu86 in BIR1 (Figure 6D) did not exist in the BIR2 model, as Glu86 is replaced by a glycine in the analogous position (Gly269) (Figure 7D). Arg5 appeared to exhibit some electro-repulsion with Arg260 and Arg262 in BIR2, and thus may account for the reduced affinity of Δ79-dOmi for BIR2 compared to Rpr and Hid (Figure 7C and D). Collectively, the biochemical and structural data indicate that Δ79-dOmi can selectively displace DRONC from the BIR2 domain in DIAP1. However, this interaction is insufficient, on its own, to induce significant levels of cell death, perhaps because the BIR1 domain retains its ability to inhibit the effector caspase, DrICE. Indeed, we have previously shown in human cells that the linker-BIR2 domain in XIAP can inhibit the effector caspase-3 and prevent cell death, even when mutations in its BIR3 domain prevent inhibition of the initiator caspase-9 (Bratton *et al*, 2002).

dOmi alleviates DIAP1 inhibition of caspases by proteolytically degrading DIAP1

Although wild-type dOmi clearly induced cell death in both S2 cells and the developing fly eye via its serine protease activity, it remained unclear precisely how this led to caspase activation. hOmi proteolytically degrades certain IAPs in mammalian cells, including cIAP1, cIAP2, and Bruce/Apollon (Jin *et al*, 2003; Yang *et al*, 2003), raising the possibility that dOmi might indirectly increase caspase activity, at least in part, by degrading DIAP1. We therefore examined the effects of dOmi on the expression levels of DIAP1 in S2 cells. As shown in Figure 8A, DIAP1 was largely absent from cells when coexpressed with wild-type Δ79-dOmi, Δ92-dOmi, or the IBM mutants (lanes 2, 4, 5, and 7), whereas DIAP1 was readily detected in cells coexpressing the catalytically inactive S266A mutants (lanes 3 and 6). Thus, dOmi's proteolytic activity was responsible for mediating the loss in DIAP1, independent of its IBMs. We next incubated recombinant dOmi with DIAP1 (immunoprecipitated from transfected S2 cells) and found that both Δ79-dOmi and Δ92-dOmi directly degraded DIAP1 in

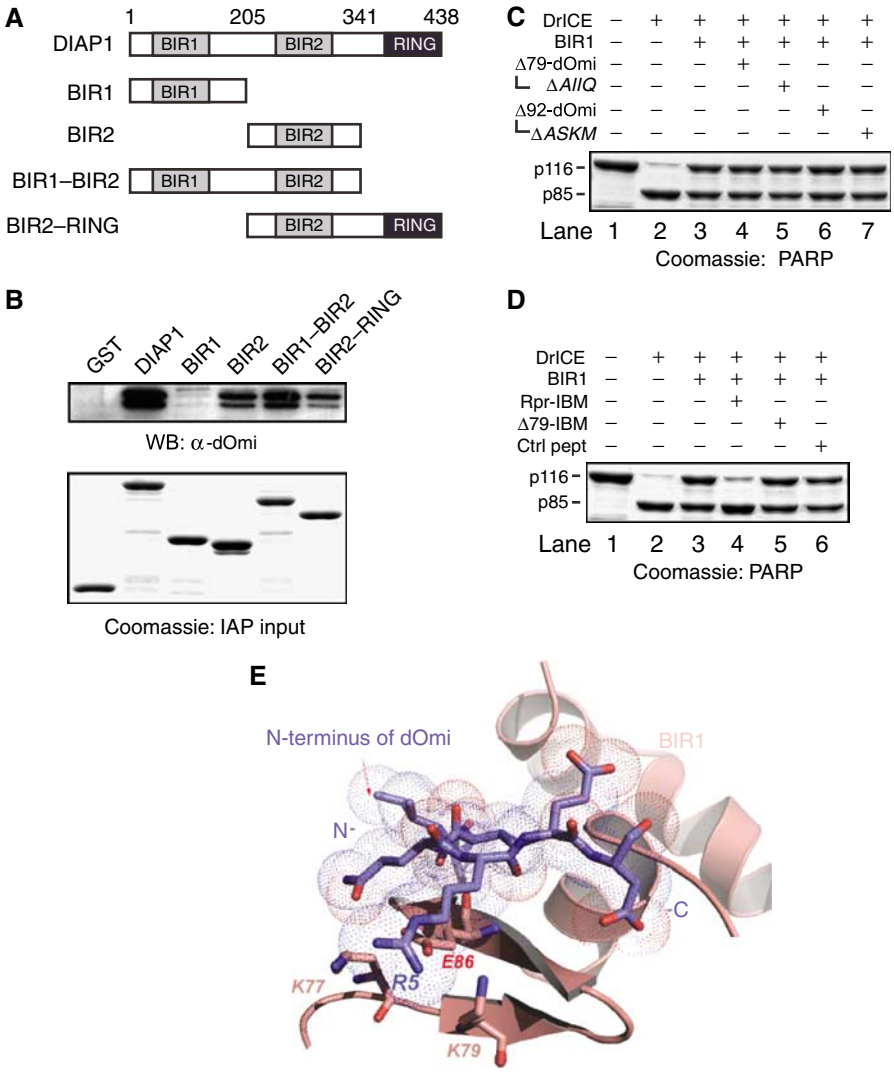

Figure 6 Mature dOmi does not bind to the BIR1 domain in DIAP1 or displace the effector caspase DrICE. (**A, B**) GST-DIAP1 and truncation mutants were expressed in bacteria and purified to homogeneity. The proteins (500 nM) were then captured using GSH–Sepharose beads and incubated (3 h at 4°C) with naïve S2 cell lysates (100 μg), in a final volume of 300 μl. The bead complexes were subsequently isolated, separated by SDS–PAGE, and immunoblotted using a rabbit anti-dOmi polyclonal antibody. (**C**, **D**) Recombinant DrICE (175 nM) was preincubated with or without GST-BIR1 (inhibitor, 3.5 μM) for 30 min at 25°C. Human PARP (substrate, 5.75 μM) was then added alone, or in combination with recombinant Δ79-dOmi, Δ92-dOmi, or the IBM truncation mutants (Δ*AIIQ*, Δ*ASKM*) (4.5 μM), and were further incubated for 60 min at 25°C. The Δ79-IBM peptide and the positive control, Rpr-IBM peptide (5 μg), were also tested in separate incubations. All protein complexes were separated by SDS–PAGE, and the gels stained with Coomassie Blue. (**E**) Structural model of Δ79-IBM bound to DIAP1-BIR1.

a concentration-dependent manner (Figure 8B). However, it was difficult to visualize many of the DIAP1 fragments, due to proteolytic removal of the HA tag. Therefore, we repeated our *in vitro* cleavage assay by incubating recombinant dOmi with GST-DIAP1 that was first purified and then biotinylated. Under these conditions, dOmi once again proteolytically processed DIAP1 into numerous fragments that were readily visualized by blotting with streptavidin-HRP (Figure 8C).

As previously noted, a number of recent studies have suggested that other IAP antagonists in the fly may stimulate DIAP1 autoubiquitinylation and target DIAP1 for destruction by the 26S proteasome (Hays *et al*, 2002; Holley *et al*, 2002; Ryoo *et al*, 2002; Wing *et al*, 2002; Yoo *et al*, 2002). dOmi, on the other hand, did not appear to induce DIAP1 autoubiquitinylation, since neither Δ79-dOmi^{S266A} nor Δ92-dOmi^{S266A} induced a loss in DIAP1, when coexpressed in S2 cells (Figure 8A, lanes 1, 3, and 6). Furthermore, in subsequent *in vitro* assays using fly embryo lysates, neither recombinant dOmi, nor the Δ79-IBM peptide, enhanced (or suppressed) the basal level of DIAP1 autoubiquitinylation (data not shown). Thus, dOmi promoted caspase activity and cell death, at least in part by ridding the cell of DIAP1. However, dOmi accomplished this feat, not by stimulating DIAP1 autoubiquitinylation, but rather by directly degrading DIAP1.

Discussion

The role of mitochondria in fly apoptosis remains highly controversial, due in large part to disagreement over whether mitochondria undergo losses in Δψm and MOMP following

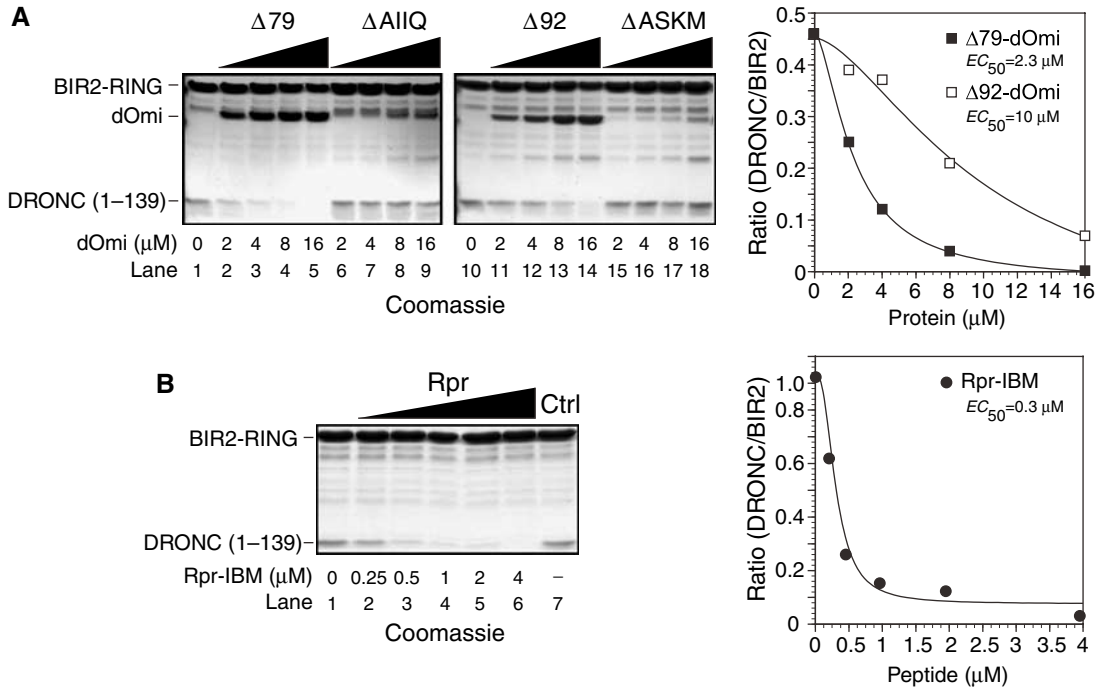

C

IAP antag. / caspase	K_d (μM) DIAP1-BIR2	XIAP-BIR3
Δ79-dOmi	0.27[a]	
Δ92-dOmi	1.18[a]	
Reaper	0.036[a]	
Hid	0.041[b]	
DRONC	0.80[b]	
Smac		0.42[c]
Caspase-9		0.74[c]

a Calculated using the Cheng–Prusoff equation and the EC_{50} values obtained in panels A and B.
b Determined in *Chai, et al.*
c Determined in *Liu, et al.*

D

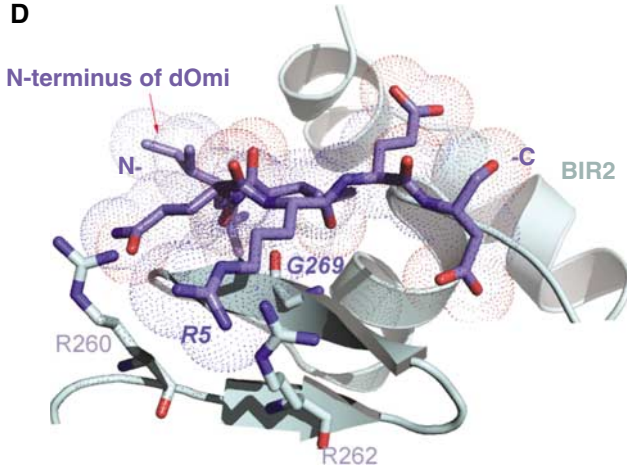

Figure 7 Mature dOmi binds selectively to the BIR2 domain in DIAP1 and displaces the initiator caspase DRONC. (**A**, **B**) GST-BIR2-RING (3 μM) was incubated with an N-terminal fragment of DRONC (6 μM), in the absence or presence of the Rpr-IBM peptide (0–4 μM), recombinant Δ79-dOmi, Δ92-dOmi, or their corresponding IBM mutants (Δ*AIIQ*, Δ*ASKM*) (2–16 μM). The dOmi proteins also contained an active-site mutation (S266A), to ensure that dOmi's proteolytic activity did not interfere with the displacement of DRONC. Displacement curves were plotted to determine the EC_{50} values for each of the Rpr-IBM peptide and dOmi proteins. All protein complexes were then separated by SDS–PAGE, and the gels stained with Coomassie Blue. (**C**) Comparison of the dissociation constants for specific fly and mammalian IAP antagonists and initiator caspases with their respective IAPs. (**D**) Structural model of Δ79-IBM bound to DIAP1-BIR2.

stress (Kanuka *et al*, 1999; Zimmermann *et al*, 2002; Dorstyn *et al*, 2004; Senoo-Matsuda *et al*, 2005). Moreover, although mitochondrial release of cytochrome *c* in mammalian cells initiates formation of the Apaf-1 apoptosome complex and activation of caspases (Cain *et al*, 2002), there is disagreement over the importance of cytochrome *c* for promoting cell death in flies (Zimmermann *et al*, 2002; Arama *et al*, 2003, 2006; Dorstyn *et al*, 2004; Mendes *et al*, 2006). The cytochrome *c* debate notwithstanding, there are additional mitochondrial proteins in mammals that play a role in promoting apoptosis, including the dual IAP antagonist and serine protease, Omi/HtrA2 (Hegde *et al*, 2001; Martins *et al*, 2001; Suzuki *et al*, 2001; Verhagen *et al*, 2001). In our studies, we set out to determine if the *Drosophila* homologue of Omi might likewise participate in cell death. We found that dOmi was highly homologous to hOmi, particularly within the serine protease domain, and that its expression was developmentally regulated. dOmi was imported into fly mitochondria and processed *in situ*, resulting in the removal of its MTS and exposure of two distinct IBMs. The mature forms of dOmi were then released into the cytoplasm following stress, through both caspase-dependent and -independent processes. However, once in the cytosol, dOmi induced cell death in S2 cells and in the developing fly eye, primarily through proteolytic degradation of DIAP1 and likely other substrates.

Indeed, catalytically inactive Δ79-dOmi^{S266A} and Δ92-dOmi^{S266A} failed to induce significant apoptosis, which

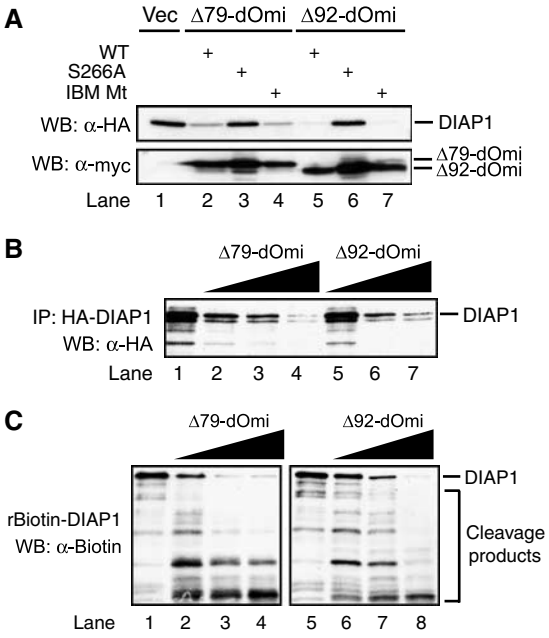

Figure 8 dOmi proteolytically degrades DIAP1. (**A**) S2 cells were cotransfected with pIE1-HA-DIAP1, along with pRmHa3-dOmi (*Δ79-dOmi*, *Δ92-dOmi*), catalytically inactive mutants of dOmi (*Δ79-dOmi*^{S266A}, *Δ92-dOmi*^{S266A}), or IBM mutants of dOmi (*Δ79-dOmi*^{GGIQ}, *Δ92-dOmi*^{GGKM}). Following the addition of CuSO4 (0.7 mM) to induce expression of dOmi and its mutants, whole-cell lysates were immunoblotted for DIAP1 and dOmi expression levels. (**B**) HA-DIAP1 was expressed in S2 cells and immunoprecipitated using an anti-HA antibody (262K, Cell Signaling). The immunoprecipitates were then incubated with wild-type Δ79-dOmi or Δ92-dOmi (50–200 nM) for 2 h at 37°C and subsequently immunoblotted for HA-DIAP1. (**C**) Biotinylated GST-DIAP1 (250 ng) was incubated with recombinant Δ79-dOmi or Δ92-dOmi (50–200 nM) for 2 h at 37°C, in a total volume of 30 μl, and subsequently blotted with streptavidin–HRP.

was somewhat surprising, given that both forms of dOmi selectively bound to the BIR2 domain in DIAP1 and displaced the initiator caspase DRONC. In particular, the affinity of Δ79-dOmi for BIR2 ($K_d \sim 0.27$ μM) was lower than that observed for Rpr-IBM ($K_d \sim 0.036$ μM), but was slightly higher than that observed for mature Smac with XIAP-BIR3 ($K_d \sim 0.42$ μM) (Liu *et al*, 2000; Wu *et al*, 2001). So why did dOmi require its proteolytic activity to induce cell death, rather than inducing rapid IBM-dependent apoptosis? Notably, unlike other fly IAP antagonists, which exhibit partial preference for either the BIR1 or BIR2 domains, dOmi completely failed to bind the BIR1 domain in DIAP1 and did not displace the active effector caspase DrICE. Thus, it is possible that the continued inhibition of DrICE by DIAP1 was sufficient to inhibit cell death. There is precedence for such a scenario in mammals, as we have previously shown that XIAP mutants that fail to bind and inhibit caspase-9 can still prevent apoptosis through inhibition of caspase-3 alone (Bratton *et al*, 2002).

One of the primary differences between fly and mammalian IAP antagonists relates to their abilities to independently induce apoptosis. Indeed, Rpr, Hid, and Grim induce robust cell death in both cultured cells and flies (Kornbluth and White, 2005), whereas overexpression of mature Smac in the cytoplasm of mammalian cells generally fails to induce apoptosis in the absence of an accompanying prodeath stimulus (Du *et al*, 2000; Creagh *et al*, 2004). A potential explanation for these results may involve their relative capacities to induce RING-dependent autoubiquitinylation upon binding to IAPs. Indeed, while many IAP antagonists in the fly induce DIAP1 autoubiquitinylation, Smac appears to suppress XIAP autoubiquitinylation (Creagh *et al*, 2004). In our studies, dOmi failed to induce or suppress DIAP1 autoubiquitinylation upon binding to its BIR2 domain. Thus, in the absence of dOmi's proteolytic activity, DIAP1 may again be free to maintain its inhibition of DrICE via its BIR1 domain. By contrast, given that DIAP1 can protect cells by targeting active DRONC for proteosomal degradation (Wilson *et al*, 2002), it is also plausible that DIAP1 might regulate cell death, in part by, promoting the turnover of dOmi. Hay and co-workers have previously reported that the DIAP1 binding mutant, DRONC (F118E), induces significantly more cell death than wild-type DRONC, when expressed in the developing fly eye (Chai *et al*, 2003), and correspondingly, we found that Δ92-dOmi consistently produced a more severe phenotype than Δ79-dOmi, in accordance with their relative affinities for DIAP1.

Others have reconciled such differences between the mammalian and fly IAP antagonists by arguing that, in contrast to the Apaf-1·caspase-9 apoptosome complex, the DARK·DRONC apoptosome complex is constitutively active. Consequently, DIAP1 is required to continuously ubiquitinylate DRONC and mediate its turnover in order to prevent cell death (Muro *et al*, 2002). In this model, Rpr, Hid, or Grim need only displace this active DRONC, in order to promote the activation of effector caspases and induce apoptosis. However, recent studies suggest that, at least for Rpr and Grim, the C-terminus of these IAP antagonists play important roles in promoting both mitochondrial injury and/or inhibition of protein translation (Claveria *et al*, 2002; Holley *et al*, 2002). These alternative functions for Rpr and Grim may be necessary to first initiate caspase activation, after which the IBMs serve to displace these active caspases from DIAP1. Therefore, it could be that binding of dOmi to DIAP1-BIR2 *per se* does not induce apoptosis, because in the absence of another stimulus, there may be very little active DRONC to displace. In any event, regardless of whether dOmi induces cell killing solely through its proteolytic activity, or functions as a pure IAP antagonist in certain contexts, our studies suggest that mitochondria may play a far more important role in apoptosis in the fly than previously thought.

Materials and methods

Bacterial and fly expression constructs

Full-length and truncated dOmi constructs were PCR amplified from an EST (AT14262; BDGP), using *Pfu* polymerase (Stratagene), and cloned into pRmHa3-myc (*Eco*RI–*Bam*HI), pUAS (*Eco*RI–*Xho*I), or pET21b (*Nde*I–*Xho*I, Novagen) vectors for expression in *Drosophila* S2 cells, flies, and *Escherichia coli* strain BL21(DE3), respectively. Active-site (S266A), IBM, and cleavage-site mutations were introduced by site-directed mutagenesis (QuikChange®, Stratagene). Similarly, the fly caspases, DRONC (residues 1–139) and full-length DrICE, were PCR amplified from ESTs (LD28292 and GH24292; BDGP) and cloned into the *Nde*I–*Xho*I and *Nco*I–*Xho*I sites of pET21b and pET28b, respectively. Full-length DIAP1 was generated by SOE-PCR using an EST (L49440) and a *thread* construct (kindly provided by Dr Colin S Duckett). DIAP1 and various truncations were then PCR amplified and cloned into pIE1-HA (*Bam*HI–*Not*I, Novagen) or pGEX-4T-1 (*Eco*RI–*Not*I, Pharmacia) vectors for expression in S2 cells and *E. coli*, respectively.

Cell culture, transfections, and cell death assays

Drosophila S2 cells were routinely cultured at 28°C in HyQ SFX-Insect medium (Hyclone) supplemented with Glutamax (20 mM, Invitrogen). For transfections, $\sim 3 \times 10^6$ cells were transfected (Cellfectin, 10 μl, Invitrogen) with pRmHa3-myc plasmid DNA (1.5–2.0 μg) encoding either wild-type, truncated, or mutant Δ79-dOmi or Δ92-dOmi proteins. For cell death experiments, cells were also cotransfected with pPAC-3-GFP (0.5 μg) and then split 24 h post-transfection into multiwell-12 plates. Protein expression was then induced with $CuSO_4$ (0.7 mM), in the presence or absence of Z-VAD-fmk (50 μM, Biomol). Cell death was assessed by flow cytometry (Beckman-Coulter FC500; $\lambda_{ex}/\lambda_{em} = 488/525$ nm) at various time points by quantifying the percentage of intact GFP^+ cells in the induced versus uninduced cell populations (i.e. $[1-(GFP^+_{induced}/GFP^+_{uninduced})] \times 100$). The expression levels of dOmi and the various mutants were confirmed by Western blotting with a mouse anti-myc antibody (9B11, Cell Signaling).

Drosophila genetics

Transgenic flies were generated by the Transgenic Fly Core Facility of the Cutaneous Biology Research Center at Massachusetts General Hospital. Seven lines for UAS-Δ79-dOmi and nine lines for UAS-Δ92-dOmi were crossed to GMR-gal4 and scored for lethality and eye phenotypes, at 25°C. To score for suppression by p35, flies of the genotype *UAS-p35/GMR-gal4; UAS-dOmi/TM6B* were compared to *SM1/GMR-gal4; UAS-dOmi/TM6B*.

Supplementary data

Supplementary data are available at *The EMBO Journal* Online (http://www.embojournal.org).

Acknowledgements

We thank Dr Janice Fischer for helpful advice, Dr John Sisson for fly embryos and antibodies to BiP, and Professor Hung-wen Liu and Zhihua Tao for recombinant PARP. This work was supported in part by start-up funds from The University of Texas at Austin, a grant from The American Cancer Society (RSG-05-029-01-CCG), and a Research Starter Grant from the Pharmaceutical Research and Manufacturers of America Foundation (all to SBB); BP was supported by the Massachusetts Biomedical Research Council Tosteson postdoctoral fellowship, and KW was supported in part by NIH grant GM55568.

References

Arama E, Agapite J, Steller H (2003) Caspase activity and a specific cytochrome *c* are required for sperm differentiation in *Drosophila*. *Dev Cell* **4:** 687–697

Arama E, Bader M, Srivastava M, Bergmann A, Steller H (2006) The two *Drosophila* cytochrome *c* proteins can function in both respiration and caspase activation. *EMBO J* **25:** 232–243

Bratton SB, Lewis J, Butterworth M, Duckett CS, Cohen GM (2002) XIAP inhibition of caspase-3 preserves its association with the Apaf-1 apoptosome and prevents CD95- and Bax-induced apoptosis. *Cell Death Differ* **9:** 881–892

Cain K, Bratton SB, Cohen GM (2002) The Apaf-1 apoptosome: a large caspase-activating complex. *Biochimie* **84:** 203–214

Chai J, Yan N, Huh JR, Wu JW, Li W, Hay BA, Shi Y (2003) Molecular mechanism of Reaper-Grim-Hid-mediated suppression of DIAP1-dependent Dronc ubiquitination. *Nat Struct Biol* **10:** 892–898

Claveria C, Caminero E, Martinez AC, Campuzano S, Torres M (2002) GH3, a novel proapoptotic domain in *Drosophila* Grim, promotes a mitochondrial death pathway. *EMBO J* **21:** 3327–3336

Creagh EM, Murphy BM, Duriez PJ, Duckett CS, Martin SJ (2004) Smac/DIABLO antagonizes ubiquitin ligase activity of inhibitor of apoptosis proteins. *J Biol Chem* **279:** 26906–26914

Danial NN, Korsmeyer SJ (2004) Cell death: critical control points. *Cell* **116:** 205–219

Dorstyn L, Mills K, Lazebnik Y, Kumar S (2004) The two cytochrome *c* species, DC3 and DC4, are not required for caspase activation and apoptosis in *Drosophila* cells. *J Cell Biol* **167:** 405–410

Du C, Fang M, Li Y, Li L, Wang X (2000) Smac, a mitochondrial protein that promotes cytochrome *c*-dependent caspase activation by eliminating IAP inhibition. *Cell* **102:** 33–42

Fuentes-Prior P, Salvesen GS (2004) The protein structures that shape caspase activity, specificity, activation and inhibition. *Biochem J* **384:** 201–232

Goyal L, McCall K, Agapite J, Hartwieg E, Steller H (2000) Induction of apoptosis by *Drosophila* reaper, hid and grim through inhibition of IAP function. *EMBO J* **19:** 589–597

Hay BA, Wassarman DA, Rubin GM (1995) *Drosophila* homologs of baculovirus inhibitor of apoptosis proteins function to block cell death. *Cell* **83:** 1253–1262

Hays R, Wickline L, Cagan R (2002) Morgue mediates apoptosis in the *Drosophila melanogaster* retina by promoting degradation of DIAP1. *Nat Cell Biol* **4:** 425–431

Hegde R, Srinivasula SM, Zhang Z, Wassell R, Mukattash R, Cilenti L, DuBois G, Lazebnik Y, Zervos AS, Fernandes-Alnemri T, Alnemri ES (2001) Identification of Omi/HtrA2 as a mitochondrial apoptotic serine protease that disrupts inhibitor of apoptosis protein–caspase interaction. *J Biol Chem* **277:** 432–438

Holley CL, Olson MR, Colon-Ramos DA, Kornbluth S (2002) Reaper eliminates IAP proteins through stimulated IAP degradation and generalized translational inhibition. *Nat Cell Biol* **4:** 439–444

Igaki T, Miura M (2004) Role of Bcl-2 family members in invertebrates. *Biochim Biophys Acta* **1644:** 73–81

Jin S, Kalkum M, Overholtzer M, Stoffel A, Chait BT, Levine AJ (2003) CIAP1 and the serine protease HTRA2 are involved in a novel p53-dependent apoptosis pathway in mammals. *Genes Dev* **17:** 359–367

Kanuka H, Sawamoto K, Inohara N, Matsuno K, Okano H, Miura M (1999) Control of the cell death pathway by Dapaf-1, a *Drosophila* Apaf-1/CED-4- related caspase activator. *Mol Cell* **4:** 757–769

Kornbluth S, White K (2005) Apoptosis in *Drosophila*: neither fish nor fowl (nor man, nor worm). *J Cell Sci* **118:** 1779–1787

Li W, Srinivasula SM, Chai J, Li P, Wu JW, Zhang Z, Alnemri ES, Shi Y (2002) Structural insights into the pro-apoptotic function of mitochondrial serine protease HtrA2/Omi. *Nat Struct Biol* **9:** 436–441

Lisi S, Mazzon I, White K (2000) Diverse domains of THREAD/DIAP1 are required to inhibit apoptosis induced by REAPER and HID in *Drosophila*. *Genetics* **154:** 669–678

Liu Z, Sun C, Olejniczak ET, Meadows RP, Betz SF, Oost T, Herrmann J, Wu JC, Fesik SW (2000) Structural basis for binding of Smac/DIABLO to the XIAP BIR3 domain. *Nature* **408:** 1004–1008

Martins LM, Iaccarino I, Tenev T, Gschmeissner S, Totty NF, Lemoine NR, Savopoulos J, Gray CW, Creasy CL, Dingwall C, Downward J (2001) The serine protease Omi/HtrA2 regulates apoptosis by binding XIAP through a Reaper-like motif. *J Biol Chem* **277:** 439–444

Means JC, Muro I, Clem RJ (2006) Lack of involvement of mitochondrial factors in caspase activation in a *Drosophila* cell-free system. *Cell Death Differ* **13:** 1222–1234

Meier P, Silke J, Leevers SJ, Evan GI (2000) The *Drosophila* caspase DRONC is regulated by DIAP1. *EMBO J* **19:** 598–611

Mendes CS, Arama E, Brown S, Scherr H, Srivastava M, Bergmann A, Steller H, Mollereau B (2006) Cytochrome *c–d* regulates developmental apoptosis in the *Drosophila* retina. *EMBO Rep* **7:** 933–939

Muro I, Hay BA, Clem RJ (2002) The *Drosophila* DIAP1 protein is required to prevent accumulation of a continuously generated, processed form of the apical caspase DRONC. *J Biol Chem* **277:** 49644–49650

Olson MR, Holley CL, Gan EC, Colon-Ramos DA, Kaplan B, Kornbluth S (2003) A GH3-like domain in reaper is required for mitochondrial localization and induction of IAP degradation. *J Biol Chem* **278:** 44758–44768

Ryoo HD, Bergmann A, Gonen H, Ciechanover A, Steller H (2002) Regulation of *Drosophila* IAP1 degradation and apoptosis by reaper and ubcD1. *Nat Cell Biol* **4:** 432–438

Salvesen GS, Duckett CS (2002) IAP proteins: blocking the road to death's door. *Nat Rev Mol Cell Biol* **3:** 401–410

Senoo-Matsuda N, Igaki T, Miura M (2005) Bax-like protein Drob-1 protects neurons from expanded polyglutamine-induced toxicity in *Drosophila*. *EMBO J* **24:** 2700–2713

Suzuki Y, Imai Y, Nakayama H, Takahashi K, Takio K, Takahashi R (2001) A serine protease, HtrA2, is released from the mitochondria and interacts with XIAP, inducing cell death. *Mol Cell* **8:** 613–621

Tenev T, Zachariou A, Wilson R, Paul A, Meier P (2002) Jafrac2 is an IAP antagonist that promotes cell death by liberating Dronc from DIAP1. *EMBO J* **21:** 5118–5129

Varkey J, Chen P, Jemmerson R, Abrams JM (1999) Altered cytochrome *c* display precedes apoptotic cell death in *Drosophila*. *J Cell Biol* **144:** 701–710

Verhagen AM, Ekert PG, Pakusch M, Silke J, Connolly LM, Reid GE, Moritz RL, Simpson RJ, Vaux DL (2000) Identification of DIABLO, a mammalian protein that promotes apoptosis by binding to and antagonizing IAP proteins. *Cell* **102:** 43–53

Verhagen AM, Silke J, Ekert PG, Pakusch M, Kaufmann H, Connolly LM, Day CL, Tikoo A, Burke R, Wrobel C, Moritz RL, Simpson RJ, Vaux DL (2001) HtrA2 promotes cell death through its serine protease activity and its ability to antagonise inhibitor of apoptosis proteins. *J Biol Chem* **277:** 445–454

Wilson R, Goyal L, Ditzel M, Zachariou A, Baker DA, Agapite J, Steller H, Meier P (2002) The DIAP1 RING finger mediates ubiquitination of Dronc and is indispensable for regulating apoptosis. *Nat Cell Biol* **4:** 445–450

Wing JP, Schreader BA, Yokokura T, Wang Y, Andrews PS, Huseinovic N, Dong CK, Ogdahl JL, Schwartz LM, White K, Nambu JR (2002) *Drosophila* Morgue is an F box/ubiquitin conjugase domain protein important for grim-reaper mediated apoptosis. *Nat Cell Biol* **4:** 451–456

Wing JP, Schwartz LM, Nambu JR (2001) The RHG motifs of *Drosophila* Reaper and Grim are important for their distinct cell death-inducing abilities. *Mech Dev* **102:** 193–203

Wu JW, Cocina AE, Chai J, Hay BA, Shi Y (2001) Structural analysis of a functional DIAP1 fragment bound to grim and hid peptides. *Mol Cell* **8:** 95–104

Yan N, Wu JW, Chai J, Li W, Shi Y (2004) Molecular mechanisms of DrICE inhibition by DIAP1 and removal of inhibition by Reaper, Hid and Grim. *Nat Struct Mol Biol* **11:** 420–428

Yang QH, Church-Hajduk R, Ren J, Newton ML, Du C (2003) Omi/HtrA2 catalytic cleavage of inhibitor of apoptosis (IAP) irreversibly inactivates IAPs and facilitates caspase activity in apoptosis. *Genes Dev* **17:** 1487–1496

Yoo SJ, Huh JR, Muro I, Yu H, Wang L, Wang SL, Feldman RM, Clem RJ, Muller HA, Hay BA (2002) Hid, Rpr and Grim negatively regulate DIAP1 levels through distinct mechanisms. *Nat Cell Biol* **4:** 416–424

Zachariou A, Tenev T, Goyal L, Agapite J, Steller H, Meier P (2003) IAP-antagonists exhibit non-redundant modes of action through differential DIAP1 binding. *EMBO J* **22:** 6642–6652

Zhou L, Steller H (2003) Distinct pathways mediate UV-induced apoptosis in *Drosophila* embryos. *Dev Cell* **4:** 599–605

Zimmermann KC, Ricci JE, Droin NM, Green DR (2002) The role of ARK in stress-induced apoptosis in *Drosophila* cells. *J Cell Biol* **156:** 1077–1087